Static Pressure Losses in 6”, 8”, and 10” Non-Metallic Flexible Duct

Kevin Weaver, EIT, Graduate Research Assistant*
Charles Culp, Ph.D., P.E., ASHRAE Fellow, Associate Professor

Texas A&M University

ABSTRACT

This study measured airflow static pressure losses through non-metallic flexible ducts in compliance with ASHRAE Standard 120-1999, Methods of Testing to Determine Flow Resistance of HVAC Air Ducts and Fittings (*ASHRAE 1999*). Duct sizes of 6”, 8”, and 10” were tested in a positive pressure, blow-through configuration. An “as-built” test protocol expands the test configurations specified by Standard 120. Previous work by researchers at Lawrence Berkeley National Laboratories (LBNL) using draw-through configurations showed that the existing data for flexible duct losses exhibit errors greater than 70% from previously published data (Abushakra et. al). Results of the current tests extend the existing ASHRAE/ACCA data for flexible duct which does not include pressure loss data for flexible ducts that are compressed beyond approximately 4%. The data from this study exhibit higher pressure losses than prior ACCA or ASHRAE data. Some configurations have over ten times the pressure loss found in rigid duct or fully stretched flexible duct of the same diameter. The experimental results were utilized to create a set of loss prediction equations for flexible duct which did not previously exist. These equations utilize compression as an input variable and allow for the prediction of static pressure losses for ducts compressed between fully stretched and 45% compression.

* Kevin Weaver is now a Senior Engineer with BesTech in Dallas, Texas. Mr. Weaver performed this research as part of his MS Thesis at Texas A&M University.

This project was supported by the Air Distribution Institute, ASHRAE, Texas Utilities and Lennox Industries.

INTRODUCTION

Prior measurements of static pressure loss for flexible ducts only considered fully stretched and naturally relaxed flat configurations, which naturally contracted to about 4% with respect to the fully stretched case. Pressure loss calculation methods exist within the Air Conditioning Contractors of America (ACCA) Manual D (*ACCA 1995*). The ASHRAE Handbook – Fundamentals Chapter 35 (*ASHRAE 2005)* also contains pressure loss data, which has linear correction factors based on the percent of compression extending to 30%. Existing research by Abushakra et al. has shown the data included in the ACCA and ASHRAE Handbook references contains errors of 70%. The measurements presented in this paper extend the measurements previously taken to include fully stretched and compression values from 4% to 45%. In addition, the development of an "as-built" test protocol improves the applicability of the pressure loss data to real installations. This protocol includes board supported (flat), joist-supported with natural sag and joist-supported with full, or long-term sag. This provides a range of pressure losses which can be expected in field installations, depending upon the extent of the sag.

TEST CONFIGURATION

The data acquisition (DAQ) setup sequences and captures the measurements needed for the static pressure loss. Figure 1 shows a diagram of the test setup. ASHRAE Standard 120 requirements were used to design the system and process the data after acquisition. A computer controlled variable frequency drive (VFD) adjusts the air flow. The VFD allows for varying the fan RPM to provide a range of 50 to 600 cfm.

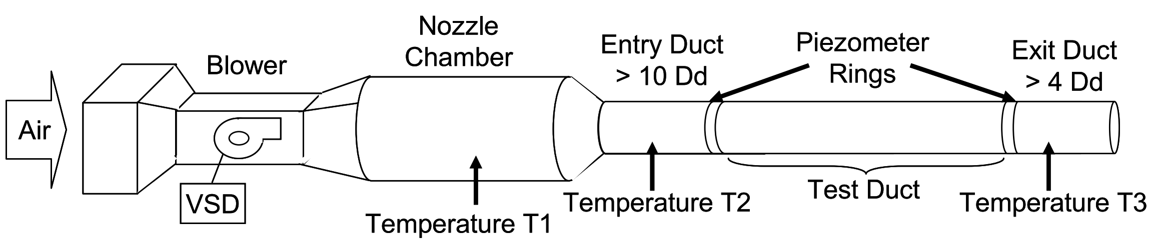

Figure 1: Test Setup

The pressure loss through the corresponding duct or fitting is then measured by an array of pressure transducers with an accuracy of ±0.25% for pressure losses of up to 0.25" H_20 and ±0.5% for pressure losses from .25" H_20 to 2.00" H_20. These 4-20 mA transducers produce a current proportional to the amount of applied pressure. A 249.0 Ω precision resistor (±0.25%) converts the current loop outputs from the sensors to voltage inputs to the DAQ. The DAQ processes the voltages and the program in the computer performs the requisite calculations and display functions.

The static pressure measurements in the test duct are performed through pressure taps set up in a piezometer ring. The ring functions as a static pressure averaging device. Each ring consists of four equally spaced and parallel connected taps. The piezometer rings meet ASHRAE Standard 120 requirements, with individual readings from each tap measuring within ±2% of one another.

The temperature measurement throughout the test run uses two silicon-junction transistor type devices, and a third 1000 Ω combination platinum temperature-humidity unit. Sensor locations are 1) at the nozzle chamber, 2) at the beginning of the test section, and 3) at the end of the test section.

Figure 1 shows the nozzle chamber upstream of the duct, per ASHRAE Standard 120. This cylindrical nozzle chamber, used for duct sizes from 4" to 10", contains a 2.5" and a 5.0" flow nozzle. Pressure taps record the pressure loss through the nozzles. The pressure transducers measure the pressure loss across the nozzles and produce the current value to the PC via the 4-20 mA loop connected to the DAQ card. The pressure loss in the nozzle is converted to mass flow rate using Equation 16 from ASHRAE Standard 120 in Section 9.3.1.7.

The automated measurement control system acquires 5,000 readings for each point reported. This occurs by taking 100 readings each second and calculating the average. Next, this process repeats 50 times with each of the 50 point values stored on disk. An average of these 50 values produces a final average value. ASHRAE validated spreadsheets were used to verify all pressure loss calculations.

AS-BUILT TEST PROTOCOL

In actual installations, duct installations occur over joists and in hung configurations. To better approximate actual installation conditions, an "as-built" test protocol using two installation configurations was created. The first, termed "board-supported", positioned a duct on top of a continuous flat horizontal board over the entire test length. The second, termed "joist–supported", replicates the duct installation over 1.5" wide supports on 24" centers. In this configuration, the duct sags between the joists when compressed and creates a test condition similar to actual installations. The natural sag test configuration occurs when the duct sags between the joists under its own weight which represents a minimal sag condition. The long-term sag condition was created by increasing the depth of the sag to represent a maximum or "worst-case" condition. Most installations will be between these test configurations.

The tests used non-metallic flexible duct with a single-helix core, an R-6 insulation layer, and a foil facing outer layer (vapor barrier). The duct testing used numerous compression ratios to provide a spectrum of data for comparison. These ratios included 0% (maximum stretch), 4%, 15%, 30%, and 45% compression. The compression ratio equals the difference between the compressed length and the maximum stretched length divided by the maximum stretched length. Setting up the compressed duct involved marking the duct in 1 foot sections when fully extended and then axially compressing to the desired ratio evenly over the length. Non-uniformities in compression increase the total pressure loss with respect to ducts with uniform compression. This approach ensures uniform longitudinal compression over the entire length of the duct under test.

The process for assembling the board-supported as-built test required uniformly compressing the duct supported by a board in a flat configuration and then performing all measurements. The process for creating the natural sag configuration required removing the board supports and letting the flexible duct sag over the 1.5” wide, 24” centered joists and then performing all measurements. Since the amount of sag can vary depending upon the installation, pressure loss measurements using two extremes of sag were measured. For natural sag, the mid-point sag distance ranges from 1” to 3” for duct compressions ranging from 4% to 45%.

Long-term sag was achieved by depressing the duct mid-point between the joists and then allowing each section between the joists to retract, emulating a longer term sag condition. Table 1 shows the approximate sag at the midpoint between the supporting joists for the natural and the long-term sag condition, measured from duct centerline to sag centerline. At duct compression below 15%, natural sag and long-term sag are equal since insufficient duct material exists to maintain a deeper sag condition. Above 30% duct compression, long-term sag will exceed natural sag as shown in Table 1. Sag creates a dramatic increase in the pressure loss through flexible duct and needs to be taken into account in any pressure loss calculation.

	Sag (inches)			
Compression	4%	15%	30%	45%
6” Flex Natural Sag	0.5”	2”	4”	7”
6” Flex Long-Term Sag	0.5”	2”	6”	11.5”
8” Flex Natural Sag	0.5”	2”	3”	4”
8” Flex Long-Term Sag	0.5”	2"	6”	7’
10” Flex Natural Sag	0.5”	1.5”	2”	3.5”
10” Flex Long-Term Sag	0.5”	1.5”	4.5”	6.5”

Table 1. Flexible Duct Midpoint Sag Lengths

The test procedure for joist and board-supported configurations exceeded the requirements in ASHRAE Standard 120-1999 (*ASHRAE 1999*) for all assembly, leak testing and measurements. Measured air property variables include ambient dry bulb temperature, barometric pressure, chamber dry bulb temperature and relative humidity, and dry bulb temperature at two points within the test duct. Measured pressure loss variables include nozzle plate static pressures, nozzle differential pressure, upstream and downstream static pressure, and test duct differential pressure.

RESULTS

The resulting data shows static pressure loss as a function of volumetric flow rate for each of the three sizes of 6”, 8”, and 10” duct. In each of the plots the static pressure loss through rigid sheet metal duct of the same diameter is presented as a comparative baseline for the results. The compression configurations tested include rigid sheet metal duct, maximum stretch flexible duct, 4% compressed flexible duct, 15% compressed flexible duct, 30% compressed flexible duct, and 45% compressed flexible duct. Each compression configuration contains data for both board and joist-supported configurations.

Rigid Sheet Metal Duct

Rigid sheet metal duct was tested for each size for agreement with existing ASHRAE / ACCA numbers (ASHRAE Handbook-Fundamentals 2005). The rigid duct was tested under the same volumetric flow rate range as the flexible duct. Resulting values for the rigid duct showed agreement to within ±5% of ASHRAE values in the 2005 Handbook.

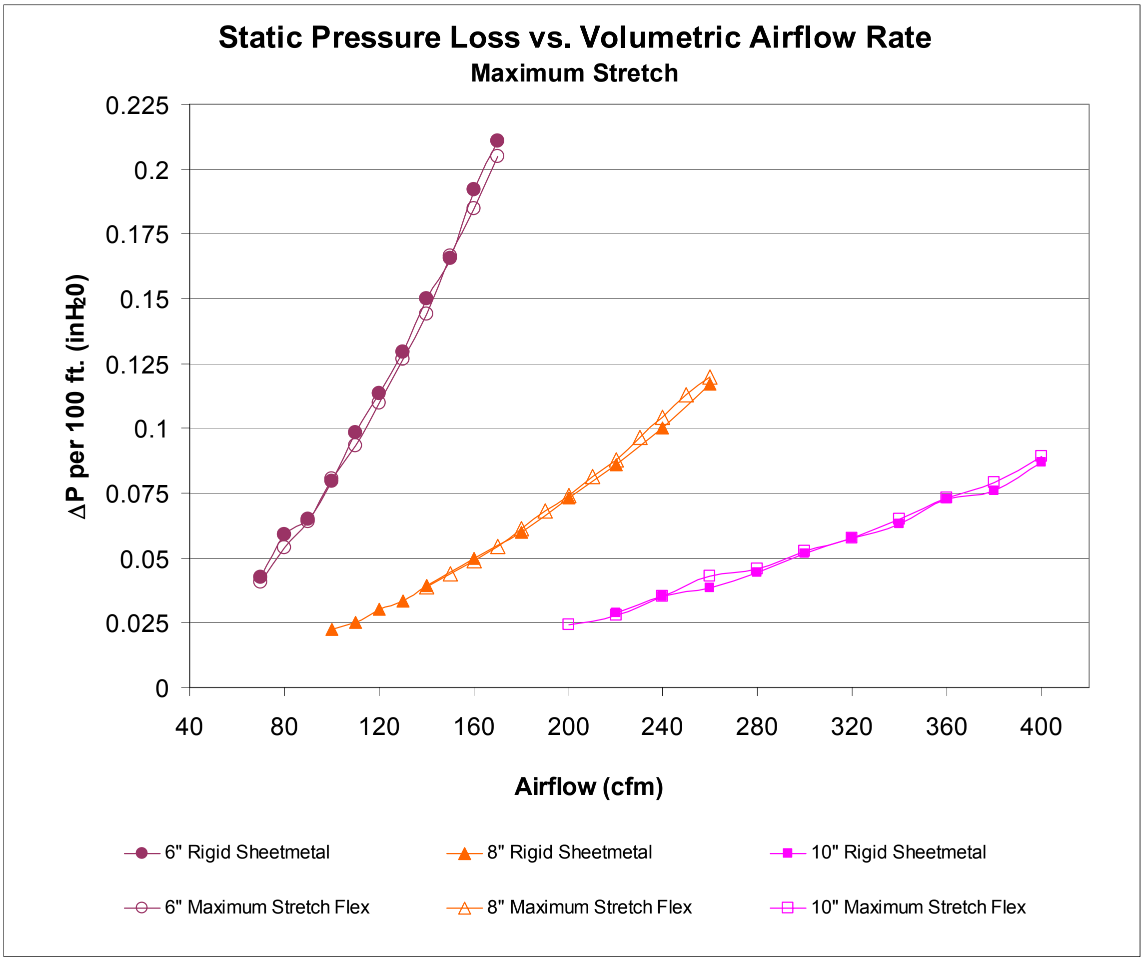

Figure 2: Static Pressure Loss in 6", 8", and 10" Non-Metallic Flexible Duct with Maximum Stretch Compared with Rigid Sheet Metal Duct

Maximum Stretch Configurations

Results for the maximum stretch case and rigid duct showed agreement within 2% as shown in Figure 2. For comparative purposes rigid sheet metal duct was tested utilizing both 3 ft. and 5 ft. standard commercially available section lengths in the 6" size. This comparative testing allows the individual contributions of transition and length to be ascertained. The resulting data showed that section length has less than a 5% effect on the static pressure loss over the measured flow range.

4% Compression Configurations

4% compression revealed substantial increases in static pressure loss as shown in Figure 3. A 4% compression rate results in 1 ft. of compression for a 25 ft. length, resulting in 25 ft. of flexible duct running 24 ft. The duct weight caused the natural sag to occur when the supporting boards were removed at the completion of the board-supported tests (flat configuration). At 4% compression, very little sag occurred. The data from the ASHRAE Handbook generally agrees with the data taken, with the condition that the Pressure Loss Correction Factor increases when the ducts sag. Some variations from experimental set-ups are expected due to the sensitivity to the pressure loss as a function of the evenness of the compression and the uniformity of sag.

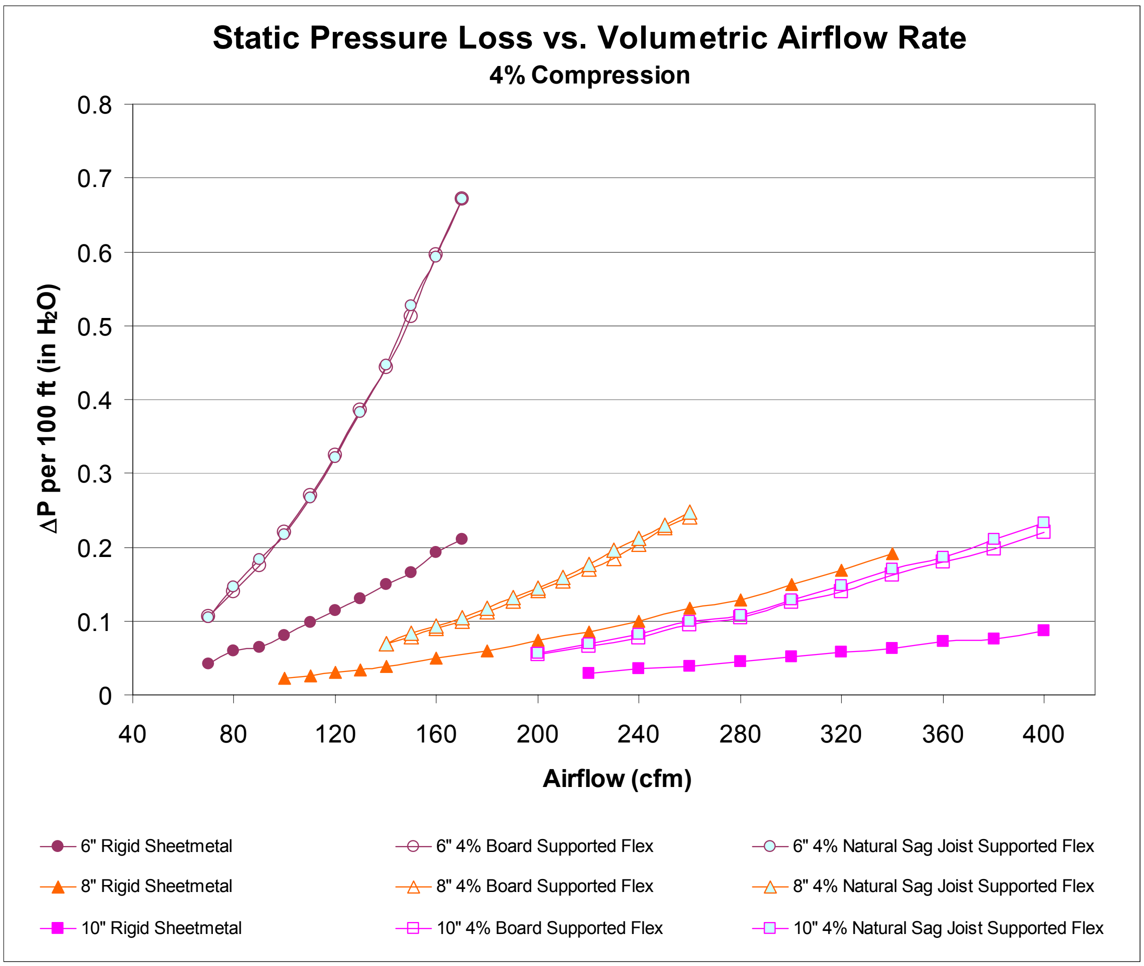

Figure 3: Static Pressure Loss in 6", 8", and 10" Non-Metallic Flexible Duct with 4% Compression Compared with Rigid Sheet Metal Duct

15% Compression Configurations

Figure 4 shows the 15% compression data. These values were found to be quite sensitive to the uniformity of the compression and variations from these values should be expected in field installations.

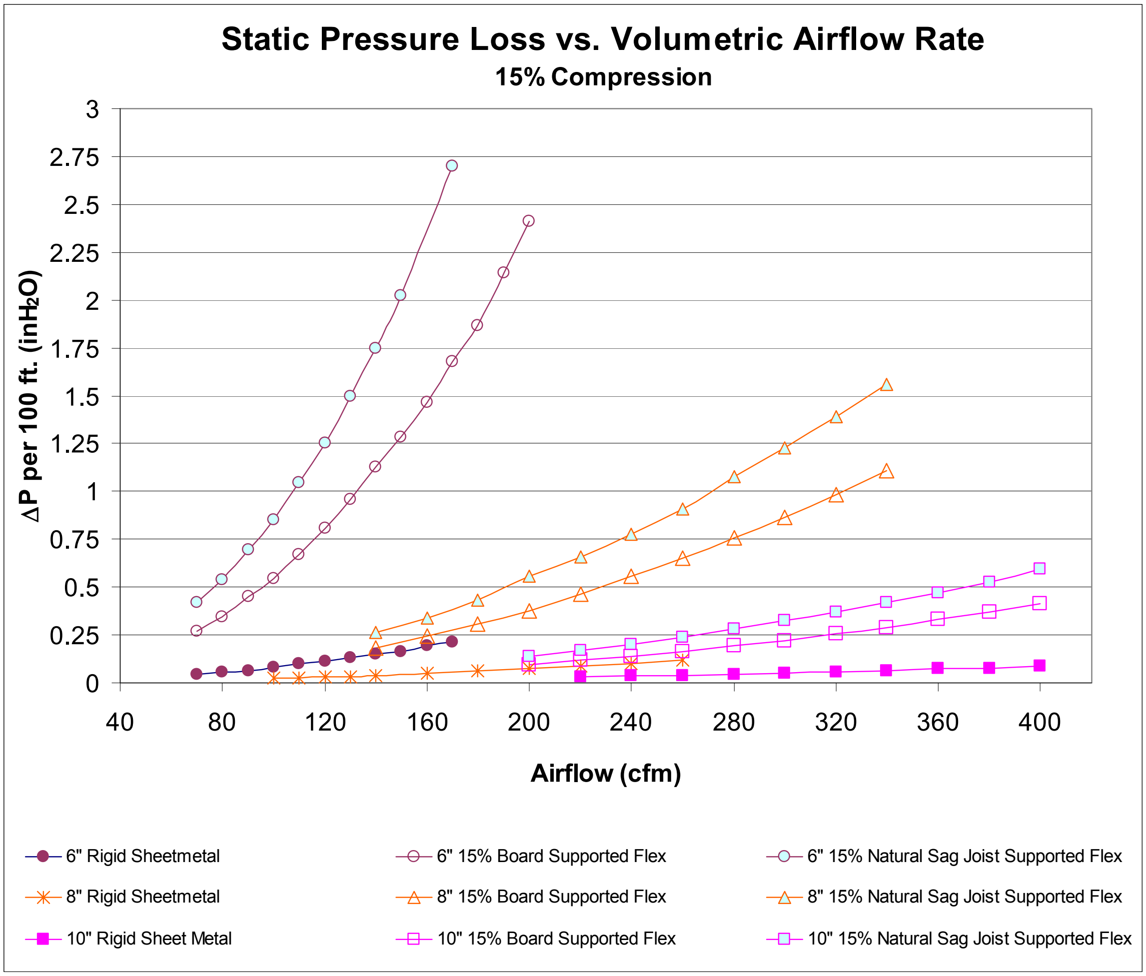

Figure 4: Static Pressure Loss in 6”, 8”, and 10” Non-Metallic Flexible Duct with 15% Compression Compared with Rigid Sheet Metal Duct

30% Compression Configurations

Figure 5 shows the 30% compression pressure loss. Again, these values were found to be quite sensitive to the uniformity of the compression.

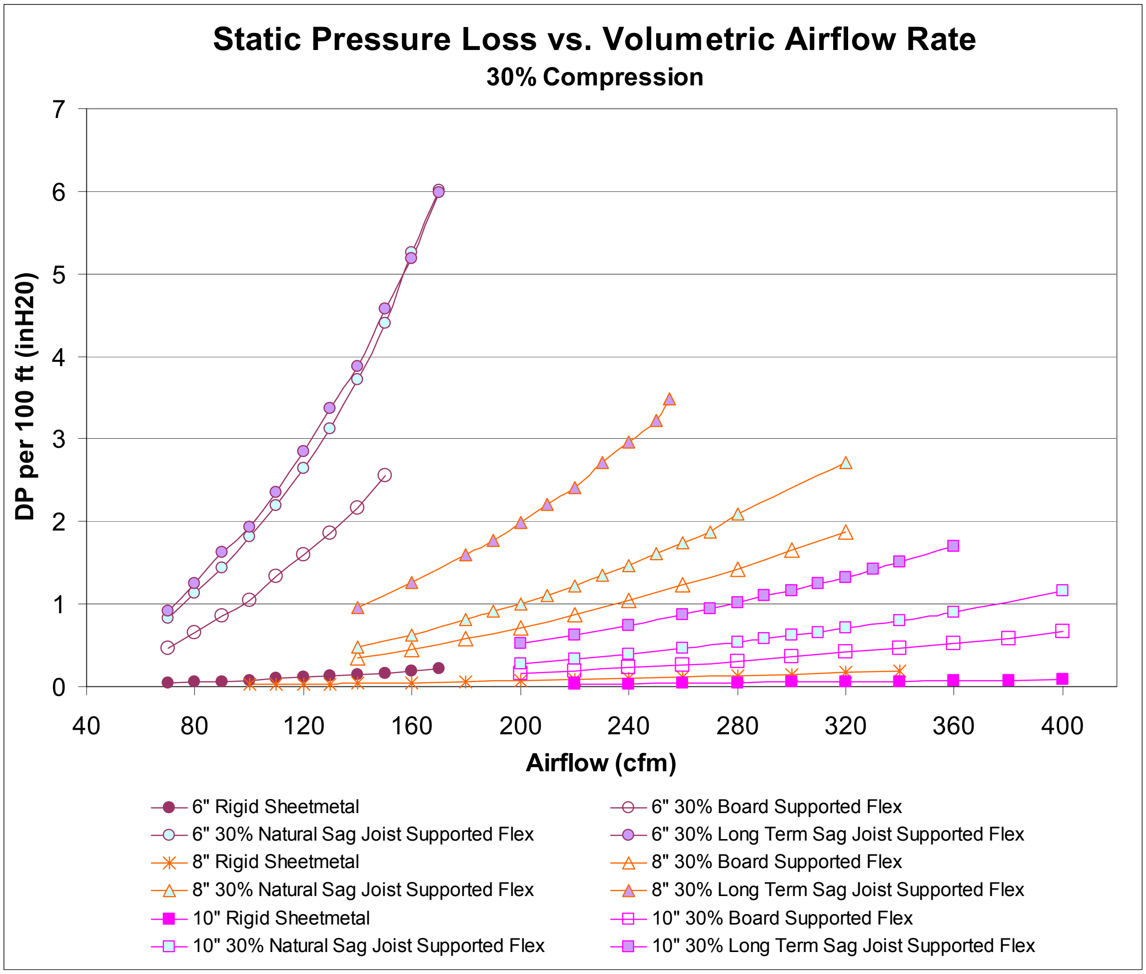

Figure 5: Static Pressure Loss in 6", 8", and 10" Non-Metallic Flexible Duct with 30% Compression Compared with Rigid Sheet Metal Duct

45% Compression Configurations

Figure 6 shows the 45% compression pressure loss.

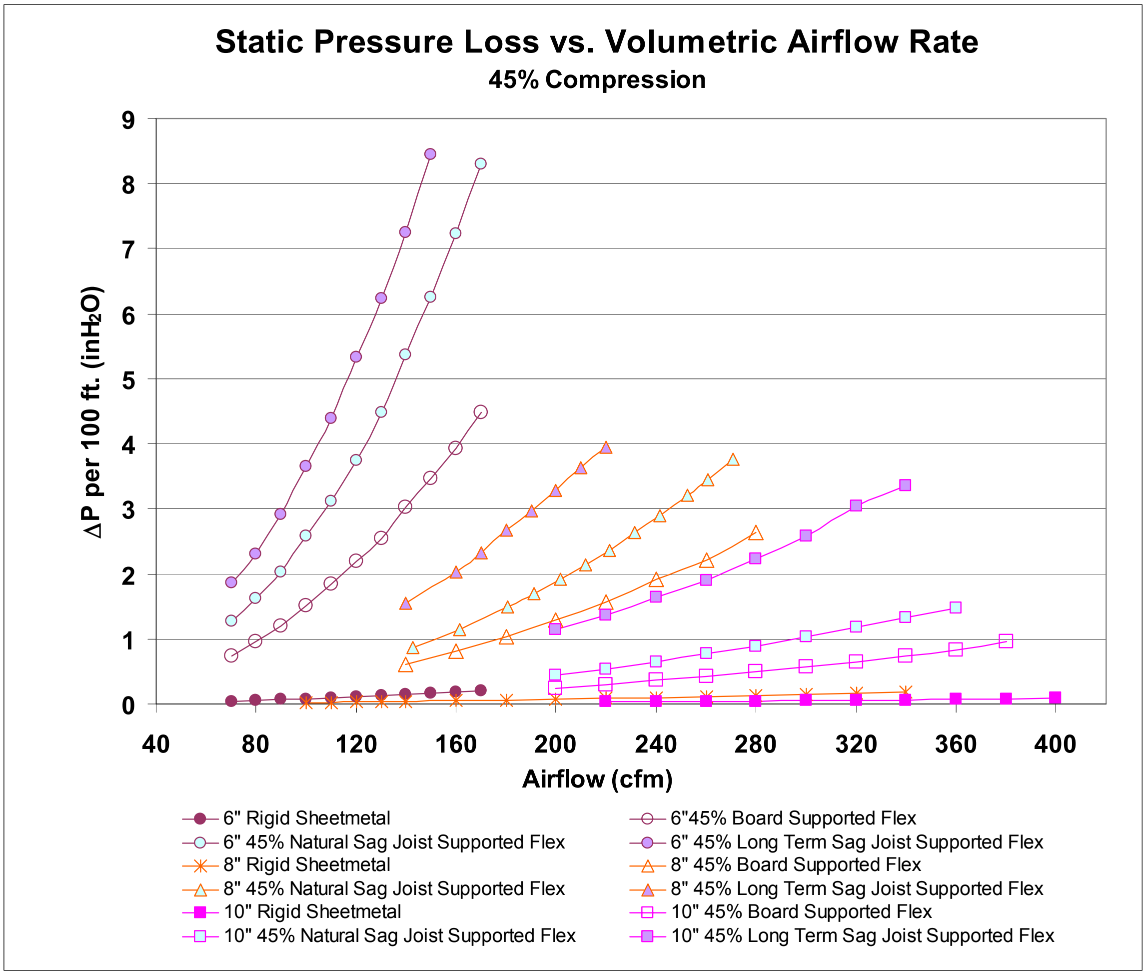

Figure 6: Static Pressure Loss in 6", 8", and 10" Non-Metallic Flexible Duct with 45% Compression Compared with Rigid Sheet Metal Duct

POWER LAW MODEL

The coefficient C and the exponent n contained are shown in Table 2 for each test compression ratio configuration. The equation has the form $P_{loss} = C * (cfm)^n$.

Size in.	Compression Ratio %	C in-H_2O/(100ft.*(cfm)^n)	n
6	Rigid Sheetmetal	1.68E-05	1.84
	Max Stretch	1.85E-05	1.82
	4% Joist-Supported	1.61E-05	2.07
	4% Board-Supported	1.47E-05	2.09
	15% Joist-Supported	4.84E-05	2.12
	15% Board-Supported	3.71E-05	2.09
	30% Joist Natural Sag	6.95E-05	2.20
	30% Joist Long Term Sag	1.33E-04	2.08
	30% Board-Supported	3.18E-05	2.26
	45% Joist Natural Sag	1.37E-04	2.14
	45% Joist Long Term Sag	3.46E-04	2.01
	45% Board-Supported	1.24E-04	2.04
8	Rigid Sheetmetal	6.23E-06	1.77
	Max Stretch	4.51E-06	1.83
	4% Joist-Supported	3.42E-06	1.98
	4% Board-Supported	2.76E-06	2.05
	15% Joist-Supported	1.21E-05	2.02
	15% Board-Supported	8.36E-06	2.03
	30% Joist Natural Sag	1.43E-05	2.10
	30% Joist Long Term Sag	2.91E-05	2.10
	30% Board-Supported	1.29E-05	2.06
	45% Joist Natural Sag	1.01E-05	2.29
	45% Joist Long Term Sag	5.56E-05	2.07
	45% Board-Supported	2.46E-05	2.05
10	Rigid Sheetmetal	1.69E-06	1.80
	Max Stretch	1.48E-06	1.84
	4% Joist-Supported	1.04E-06	2.06
	4% Board-Supported	1.21E-06	2.02
	15% Joist-Supported	2.19E-06	2.09
	15% Board-Supported	1.28E-06	2.12
	30% Joist Natural Sag	4.50E-06	2.08
	30% Joist Long Term Sag	1.15E-05	2.02
	30% Board-Supported	2.85E-06	2.06
	45% Joist Natural Sag	7.19E-06	2.08
	45% Joist Long Term Sag	2.05E-05	2.06
	45% Board-Supported	4.12E-06	2.08

Table 2. Power Law Model Data

COMPARISON WITH EXISTING DUCT CALCULATORS (DUCTULATORS)

The resulting data were compared with results achieved with a duct calculator, or ductulator, typically used by industry. A ductulator (Atco Rubber Products 1994) was published in conjunction with a slide chart. A ductulator uses input flow rate and duct size to calculate static pressure loss. The percent compression is not an input variable. These ductulator results do not include ASHRAE correction factors. Due to the nature of the visually interpolated ductulator values from the mechanical scale, some variation (on the order of ±5%) is expected between observations.

Table 3 shows the ductulator predicted pressure loss, the measured pressure loss and the error factors which occur when nominal air flows are used. The error factor listed in Table 3 is the result of the measured value divided by the ductulator value. This provides a quick indication of the magnitude of the ductulator underestimation. The chosen flow rates are representative of the typical cfm found in the listed duct sizes in residential construction. The underestimation for the 4% compression cases is within a factor of ±0.6 in-$H_2 0$ for all flow rates. The test results at 4% compression compare similarly to the ductulator values. Experimental results from the LBNL work concluded that flexible ducts naturally relax to about 4% compression when stretched and released.

	Flow	Max. Stretch	4% Joist Supported	15% Joist Supported	15% Board Supported	30% Joist Natural	30% Board Supported	45% Joist Natural	45% Board Supported
	cfm	in-$H_2 0$	in-$H_2 0$	in-$H_2 0$	in-$H_2 0$	in-$H_2 0$	in-$H_2 0$	in-$H_2 0$	in-$H_2 0$
Ductulator									
6"	100	0.155							
8"	200	0.14							
10"	300	0.095							
Measured									
6"	100	0.081	0.222	0.841	0.561	1.745	1.052	2.609	1.485
8"	200	0.073	0.123	0.537	0.382	0.974	0.718	1.878	1.288
10"	300	0.054	0.132	0.329	0.229	0.639	0.361	1.022	2.080
Error Factor									
6"	100	0.520	1.430	5.429	3.618	11.255	6.785	16.830	9.579
8"	200	0.523	0.878	3.834	2.727	6.955	5.127	13.414	9.198
10"	300	0.564	1.387	3.462	2.408	6.731	3.803	10.755	21.895

Table 3: Ductulator Prediction versus Measured Data

DEVELOPMENT OF LOSS PREDICTION EQUATIONS

The current methodology to determine the pressure loss through flexible duct involves estimating the amount of compression (L / L_{FE} – see the 2005 ASHRAE Handbook Fundamentals, page 35.7, Figure 8) and then applying the correction factors for the specified flexible duct. This method only considers straight flexible duct. This paper extends the calculations to calculate the pressure loss over a range of compression with natural sag and long-term sag exhibited by ducts installed over joists on 24” centers.

Currently no equation exists which incorporates compression as a variable that may be universally applied to flexible duct. The existing method applies ASHRAE correction factors to rigid duct data. Static pressure loss for ductwork normally uses the Power Law to express pressure loss in in-H_2O per 100 ft. This equation contains a coefficient of C, the flow rate in cfm, and some exponent, n. The value of n is normally assumed to be 2, although it fluctuates in actual applications.

In order to create a method for predicting the static pressure loss in flexible duct, the necessary input variables and constraints had to first be determined. Input variables include duct diameter (D_d, in.), flow rate (cfm), percent compression ($\%C = ((1\text{-}L)/L_{fe})$), and the amount of sag in joist-supported configurations. Constraints included standard temperature and pressure, as well as uniform compression throughout the duct length, which requires that each linear section of the duct be compressed equally compared with the other sections of the duct.

A set of predictive coefficients for the coefficient C used in the Power Law were created based on experimentally-determined data. Using these coefficients, plots and tables were created which allow for the prediction of static pressure loss (in-H_2O per 100 ft.) for various configurations and flow rates. The new coefficients correct the static pressure loss produced from the Power Law by adjusting the coefficient of C to compensate for the difference in the exponent from the traditionally assumed value of 2. These are based on assumed nominal flow rates to provide minimum error compared to the actual data. The nominal flow rates used are 100 cfm for 6" duct, 150 cfm for 8" duct, and 250 cfm for 10" duct. The exponent, n, used in the predictive equation is always 2. The % error is less than ±7% for every case within the range of ±30cfm of the nominal cfm. The calculated static pressure losses produced using the "corrective" coefficients were also compared to actual losses for flow rates outside the nominal cfm by more than 100%. In every case the resulting % error was less than 15%. The Power Law equation (Eqn. 1) is:

$$\Delta P(in - H_2 0\ per\ 100 ft.) = C * cfm^n \qquad \text{Eqn. 1}$$

Using the predictive coefficient of Ce (for C-estimated) and a value of 2 for the exponent (Eqn. 2), the predictive Power Law becomes:

$$\Delta P(in - H_2 0\ per\ 100 ft.) = Ce * cfm^2 \qquad \text{Eqn. 2}$$

With the corrective coefficients, the static pressure loss could now be accurately predicted for 6", 8" and 10" duct with compression ranging from fully stretched to 45% compression. Three configurations including board-supported (flat), natural sag, and long-term sag were chosen. The applicable corrective coefficient can be sourced from the table and then input into the power law along with cfm and the exponent of 2. This set of three equations provides the static pressure loss prediction for any compression ratio with an accuracy of ±10%.

Figure 7 shows the range of data obtained for the coefficient of C, with the three configurations using 10" flexible duct. This shows the impact of sag in determining and predicting the pressure loss under different conditions.

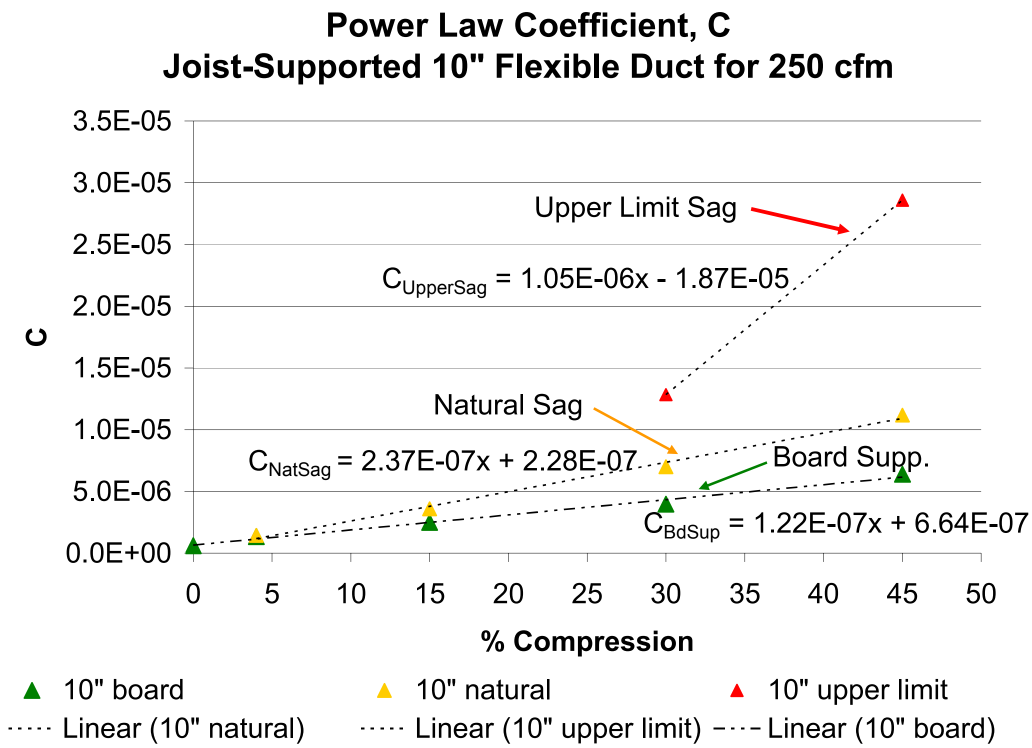

Figure 7. Example plot displaying equation of the line for each configuration

Using the extracted line equations to solve for Ce at any percent compression, a new set of plots (Figure 8) were created which display duct size on the x-axis and Ce on the y-axis. Using this data, an equation was derived for each of the three configurations - one for board-supported configurations (Eqn. 3), one for natural sag configurations (Eqn. 4), and one for long-term sag configurations (Eqn. 5).

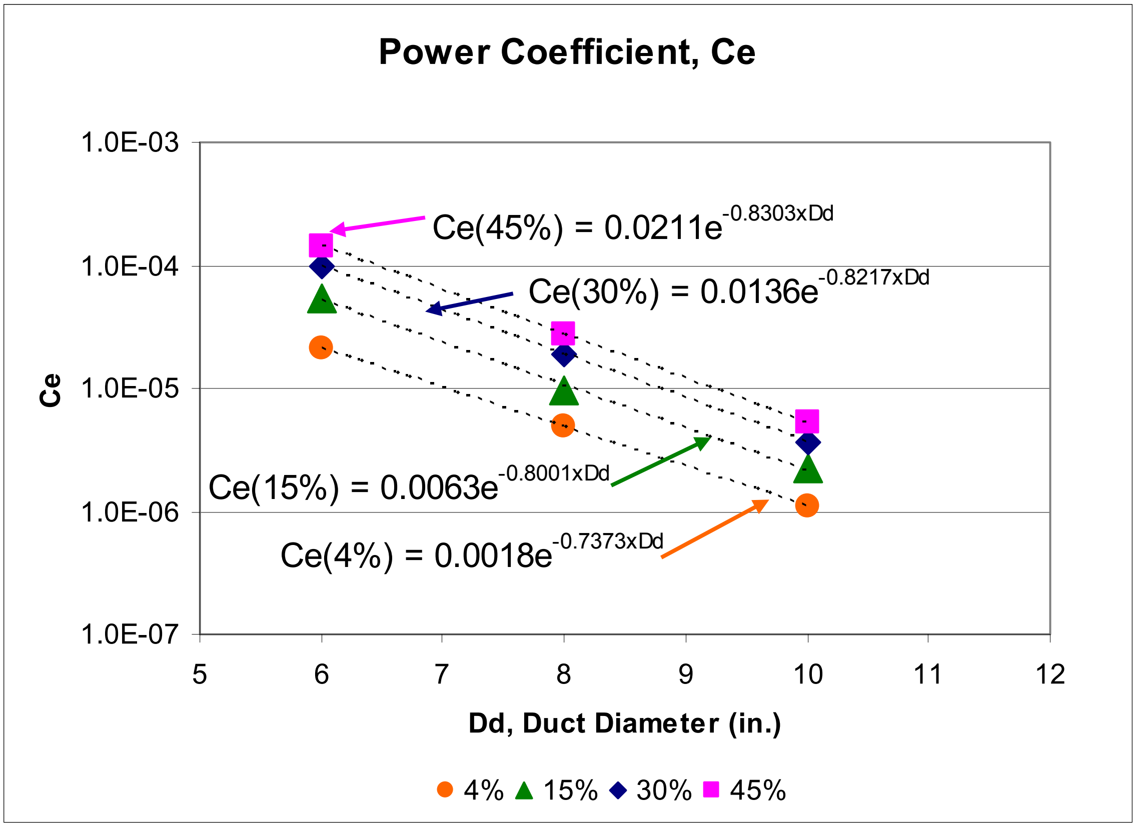

Figure 8. Corrective coefficient given duct size and percent compression

A range of static pressure loss values may now be predicted for any duct configuration. The minimum value is associated with the board-supported equation. The maximum value is associated with either the natural sag equation or the long-term sag configuration depending on percent compression. The natural sag equation can be used for percent compression under 15%, and the long-term sag equation should be used for all percent compression configurations over 15%.

Board-supported

$$C_{e,b} = (5\times10^{-4}(\%C) - 4\times10^{-4})\, e^{(-.0392LN(\%C)-.6866)*D_d} \qquad \text{Eqn. 3}$$

Natural Sag:

$$C_{e,n} = (9\times10^{-4}(\%C) - 1.9\times10^{-3})\, e^{(-.0297LN(\%C)-.7368)*D_d} \qquad \text{Eqn. 4}$$

Long-term Sag:

$$C_{e,l} = (4\times10^{-5}(\%C) + .016)\, e^{(-.74*D_d)} \qquad \text{Eqn. 5}$$

Example:

Equation 6 shows the pressure loss per 100 ft. for 15% compressed board-supported 6" flexible duct flowing 100 cfm using actual measured data, complete with the actual extracted coefficient of C and value of n:

$$\Delta P(in - H_2 0\ per\ 100 ft.) = 3.705 \times 10^{-5} \times 100^{2.09} = .561\ in - H_2 O \qquad \text{Eqn. 6}$$

Equations 7 through 11 show the calculated pressure loss per 100 ft. in 15% compressed 6" flexible duct flowing 100 cfm using empirically determined and corrected coefficient of Ce (calculated) with a standard value of 2 for n:

$$C_e = (5 \times 10^{-4(\%C)} - 4 \times 10^{-4}) e^{(-.0392 LN(\%C) - .6866) * D_d} \qquad \text{Eqn. 7}$$

$$C_e = (5 \times 10^{-4(\%C)} - 4 \times 10^{-4}) e^{(-.0392 LN(15) - .6866) * 6} \qquad \text{Eqn. 8}$$

$$C_e = 6.103 \times 10^{-5} \qquad \text{Eqn. 9}$$

$$\Delta P\ per\ 100 ft. = C_e * cfm^2 \qquad \text{Eqn. 10}$$

$$\Delta P\ per\ 100 ft. = 6.103 \times 10^{-5} * 100^2 = 0.61\ in - H_2 O \qquad \text{Eqn. 11}$$

The predictive approach yields a percentage error of 8.7% compared with the actual value of 0.561 in-H_2O. For a joist-supported duct, this value represents the minimum static pressure loss. The maximum static pressure loss could be calculated in the same manner using the equation for natural sag configurations. Using this method, a predictive range of loss for the duct may be estimated.

DISCUSSION

The results show that the change in air flow path causes a large increase in the pressure loss through the duct. When making use of the predictive equations, the effects of straightness of run and uniformity of compression must be considered. The above pressure loss prediction equations were developed based on data gathered by testing lengths of duct in a laboratory environment. The two conditions used for these tests were 1) a straight installation, with no bends or curves other than sag, and 2) uniform compression. Sag in the ductwork between support joists was accounted for, as discussed previously.

COMPARISON TO PREVIOUS WORK

A previous study (Abushakra et. al) examined the effects of compression on the static pressure loss through flexible duct. Abushakra's study tested flexible duct in a draw-through configuration with nominal compression ratios of maximum stretch, 15%, and 30%. Table 4 displays the results of the current testing and Abushakra's testing for non-sag straight ducts with 0% (maximum stretch), 15% and 30% compression. It should be noted that the current testing used a blow-through configuration while Abushakra used a draw through configuration, so the data cannot be directly compared. However, the two data sets do show similar results.

	Flow	Max. Stretch	15% Board Supported	30% Board Supported
	cfm	in-H$_2$0	in-H$_2$0	in-H$_2$0
Abushakra et.al				
6"	100	0.109	0.458	0.984
8"	200	0.078	0.308	0.498
10"	300	0.062	0.221	0.344
Weaver et. al				
6"	100	0.081	0.561	1.052
8"	200	0.073	0.382	0.718
10"	300	0.054	0.229	0.361

Table 4: Comparison to Previous Work

CONCLUSIONS

Non-metallic flexible duct pressure losses, at maximum stretch, fall within ±2% of rigid sheet metal losses. At compression values over 4%, non-metallic flexible duct exhibits 2 to 10 times increased pressure losses over sheet metal.

The experimental results also demonstrate that with compression ratios exceeding 4%, the duct performance varies considerably with slight variations in the installation. The results for the as-built test protocol need to be used as a range of values that can be encountered in field installations since non-uniform compression increases duct pressure loss above the values derived from the pressure loss equations for straight, natural sag and maximum sag configurations.

The static pressure loss prediction equations allow for the prediction of losses in straight-run flexible duct configurations of varying compression, sag, and cfm. The equations predict the static pressure loss through the duct to within ±15% error from actual experimental measurements.

ACKNOWLEDGEMENTS

This work was funded by the Air Distribution Institute, ASHRAE, Texas Utilities and Lennox Industries. We thank them for their support of this research.

REFERENCES

Abushakra, B., D. Dickerhoff, I. Walker and M. Sherman. 2002. *Laboratory Study of Pressure Losses in Residential Air Distribution Systems*. Lawrence Berkeley National Laboratory Report LBNL-49293, Berkeley, CA.

Abushakra, B., I. S. Walker, M. H. Sherman. 2004. *Compression Effects on Pressure Loss in Flexible HVAC Ducts*. International Journal of Heating, Ventilating, Air-Conditioning and Refrigeration Research, Volume 10, No. 3, pp 275 – 289.

Abushakra, B., I. S. Walker, M. H. Sherman. 2002. *Laboratory Study of Pressure Losses in Residential Air Distribution Systems*. Proc. ACEEE Summer Study 2002, American Council for an Energy Efficient Economy, Wash. D.C.

ACCA. 1995. *Residential Duct Systems. Manual D*. Air Conditioning Contractors of America. Washington, DC.

Altshul, A.D. and P.G. Kiselev. 1975. *Hydraulics and Aerodynamics*. Stroisdat Publishing House, Moscow, USSR.

ASHRAE. 2005. ASHRAE *Handbook of Fundamentals*. American Society of Heating Refrigerating and Air-conditioning Engineers, Atlanta, Georgia.

ASHRAE. 1999. *ASHRAE Standard 120P*, *Methods of Testing to Determine Flow Resistance of HVAC Air Ducts and Fittings, June 1999*. American Society of Heating Refrigerating and Air-conditioning Engineers, Atlanta, Georgia.

ASHRAE - TC 5.2. 2006. Communication with Herman Behls, Chair TC 5.2, and Bass Abushakra, Vice-Chair TC 5.2.

Atco Rubber Products, Ductulator. 1994. Fort Worth, TX

Tsal, R.J. 1989. Altshul-Tsal friction factor equation. *Heating, Piping and Air Conditioning.*